A variational framework for affine registration and segmentation with shape prior: application in echocardiographic imaging

Igor Dydenko Denis Friboulet Isabelle E. Magnin

CREATIS
INSA, Bâtiment Blaise Pascal, 69621 Villeurbanne Cedex, France
e-mail: {*dydenko, friboulet, magnin*}*@creatis.insa-lyon.fr*

Abstract

We propose a level set formulation for registration and segmentation with a shape prior. Registration of a prior contour on the image is expressed as the problem of estimating an affine transform minimizing a global region-based criterion. This registration is furthermore constrained using the available estimated inter-frame velocity field. We show that such a scheme yields consistent registration when only partial information about the shape to be registered is available. The segmentation step is then formulated through front propagation, constrained with the registered shape prior. The same region based criterion is used both for the registration and the segmentation step. The proposed approach is then specifically adapted for the segmentation of the cardiac muscle in echographic sequences. Encouraging experimental results obtained in two full echocardiographic sequences show that the proposed approach provides consistent results in terms of segmentation and stability through the cardiac cycle.

1 Introduction

Segmentation and tracking of moving tissues are of major interest in cardiac image processing. Recent advances in the field of echographic equipment enable acquisitions at very high frame rates, ranging from 150 to 350 frames per second (fps) (rates of 60 to 80 fps are common in clinical practice). In such conditions, it is possible to perform reliable estimation of the local axial tissue velocity. From this estimate, mechanical properties of the tissue, such as strain and strain rate, can be derived [5]. Their evolution through the cardiac cycle is a source of valuable information for the assessment of the myocardial viability. This task requires tracking regions of interest in the muscle, and it is currently performed manually by the cardiologist. In this context, the present paper addresses automatic segmentation of the cardiac muscle in echographic sequences, as a first step to muscle tracking. Our goal is to use the same kind of data as is available to the cardiologist (see fig. 1), that is the envelope (the usually displayed grayscale image) and the axial velocity field.

Due to attenuation, speckle noise and distortions related to the polar geometry of the acquisition, ultrasound images are known to be of a relatively poor quality [14], as compared to other medical imaging modalities. Moreover, cardiac structures do not always appear as separated and delimited objects in the echocardiographic image; during one acquisition, they may change topology, or even quit the probe's field of view.

The desire to develop a flexible method able to handle topology changes and adapted to a wide range of echocardiographic views motivated our choice of the level set representation. Although level sets have many advantages (natural handling of topology changes, ease to put in practice)[18], they are also very sensitive to noise. Therefore, we introduce prior information of two types, in two consecutive steps of processing:

1 **motion prior;** the affine model for the inter-frame motion is introduced in a registration step, and the model is further constrained by the estimated displacement data,

2 **shape and position prior;** the evolving level set is compelled to stay close to the previously registered contour in the segmentation step.

In both steps, the evolution of the contour is driven by a statistical region-based term. This region-based evolution term is directly inspired by the pioneering work of Zhu and Yuille [26], extensively used since then in the field of level sets [20, 23, 3].

The use of a prior in the level set framework has recently been proposed by several investigators [13, 24, 12, 22], and an affine motion of the prior shape was used in [4]. As opposed to most of these studies, in our approach the shape prior is not constructed from a training set, but extracted from the available data. This is motivated by the high variability of shapes and positions observed in different acquisitions of echographic cardiac data. In contrast to [4, 22], the registration of the prior shape is directly guided by the data, not by the evolving contour. The data-based registration framework which we developed can be compared to the one described in [25].

In our algorithm registration and segmentation are performed in two separate, consecutive steps. This allows us to use the registered contour not only as shape, but also as position prior, which has the advantage of preventing the level set from falling into local minima. In this sense, the idea

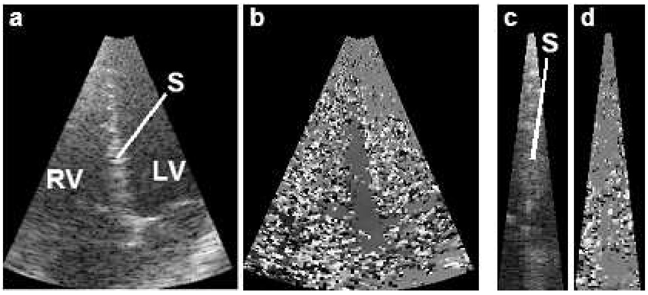

Figure 1: Example of the processed data: envelope images (a, c) and axial velocity fields (b, d). Sequence (a, b) was acquired at 145 fps, and sequence (c, d) at 322 fps

is close to the approach described in [14], which obtained the prior shape and position by segmenting the subsampled echocardiographic image.

In a closely related work, [19] introduced an affine model for the segmentation of video sequences. The transform parameters were estimated based on an optical flow constraint, and used as one of the terms driving the evolution of the level set. In contrast to this approach, we use the affine model as a mean to limit the number of degrees of freedom of the contour, and the transform parameters are estimated based on statistical region properties in a single frame. In this framework, the motion field obtained by any mean (e.g. optical flow) can be used as an additional prior on the affine transform.

Related work in the field of echographic cardiac image segmentation include an active contour guided by optical flow [15], spatio-temporal feature detection [17] and multiresolution texture segmentation [2]. The use of velocity information estimated by Doppler Tissue Imaging has been proposed to constrain segmentation [21, 16]. Similarly to the two last studies, we use the axial velocity information to constrain registration. Only recently first attempts to employ level sets for echocardiographic segmentation have been described. Proposed techniques include shape priors [4], robust 3D segmentation [1] and a multi-scale level set framework [14].

In the scope of the present work, we segment sequences acquired in the apical four chamber view. Fig. 1 presents one frame extracted from each of the processed acquisitions, along with the estimated axial (i.e. vertical in the image) velocity field. The septum (S) has been indicated in the envelope image, as well as the left and the right ventricles (LV and RV). The upper and lower limits of the septum are not clear, since on one side (the upper one on the figure) it is connected to the heart's apex and drowned in the near field of the ultrasound probe, while on the other side it is connected to the valves and the wall between the atria. It seems obvious that additional or a priori knowledge is necessary to correctly identify and track the muscle.

2 The level set framework

We use the now classical formulation of the level sets, where the closed evolving curve Γ

$$[\Gamma : [0, 1] \mapsto \Re^2, s \mapsto p = \Gamma(s)] \tag{1}$$

is embedded as the zero level set of a higher dimension embedding function, $u(p)$:

$$u(p) = \begin{cases} 0 & , p \in \Gamma \\ -D(p, \Gamma) & , p \in \Omega^{in} \\ +D(p, \Gamma) & , p \in \Omega^{out} \end{cases} \tag{2}$$

$\Omega = \Omega^{in} \cup \Omega^{out}$ is the image domain, and $D(p, \Gamma)$ is the minimum Euclidean distance between the pixel $p = (x, y)$ and the curve Γ. Suppose that the curve Γ evolves in its inward normal direction N according to a scalar function:

$$\frac{d\Gamma(s, t)}{dt} = F(\Gamma(s, t), t)N(\Gamma(s, t)) \tag{3}$$

It has been proven [18] that u has to evolve according to equation:

$$\frac{du(p, t)}{dt} = -F(p, t)|\nabla u(p, t)| \tag{4}$$

Over the last years, statistical region information has been extensively considered as an alternative to boundary information in segmentation of noisy data [20, 3]. Let $P_{in}(I(p))$, $P_{out}(I(p))$ be the probability density functions (PDF) of observing the value $I(p)$ at pixel p, in the inside and outside of the object, respectively. The problem of finding a partition of the image which maximizes the posterior probability is equivalent to finding the configuration $(\Omega_{in}, \Omega_{out})$ that minimizes the following cost functional:

$$E(\Gamma) = -\iint_{\Omega_{in}} \log P_{in}(I) d\omega - \iint_{\Omega_{out}} \log P_{out}(I) d\omega \tag{5}$$

In order for the curve to evolve in the direction which minimizes the cost (gradient descent scheme), the evolution of Γ has to follow the equation [26]:

$$\frac{d\Gamma}{dt} = -\log \frac{P_{in}(I)}{P_{out}(I)} N \tag{6}$$

This evolution of the curve will be subsequently called unconstrained evolution, and we define $\delta = \log \frac{P_{in}(I)}{P_{out}(I)} N$.

In the scope of the present work, region terms based on two different PDF are used: the Gaussian and the Rayleigh PDF.

3 Affine registration of a prior shape

The issue of extracting a prior shape roughly capturing the shape of the segmented object will be addressed in section *Results in echographic data*. At present, we suppose that such a prior shape is available, and that it is positioned in the vicinity of the object. The prior shape Γ^π is embedded as the zero level set of the signed distance map u^π, and (Γ_0^π, u_0^π) describe its initial position.

We now address the problem of positioning the prior shape on the object within the affine registration framework, in the sense of minimizing the posterior segmentation probability. In 2D, the affine transformation parameters are: the 2×2 matrix M which defines rotation, shear and scale, and the 2-component translation vector T. The affine transform of any point p is then defined as follows (all treated vectors are column vectors):

$$p' = Mp + T \tag{7}$$

We propose to perform registration by computing the affine transform ($\hat{M}, \hat{T}$) which provides the evolution the closest to the unconstrained one (as given by eq. 6), in the least square sense. Such a transform is thus the solution minimizing:

$$F_{M,T} = \int_{\Gamma^\pi} \left| v(p) + \delta(p) \right|^2 ds \tag{8}$$

where $v(p) = (v_x, v_y) = \frac{dp}{dt}$ is the displacement of point p of the contour (or of its interior $\Omega_i n$) induced by the affine transform, and the positive sign $(+)$ results from the negative in eq. 6.

If one considers the affine motion of the interface in each iteration as stationary (i.e. the motion field does not depend on time t), and also supposing without loss of generality that the time step in each iteration is 1, the motion field at each point p expresses as follows:

$$v(p) = (M - I)p + T \tag{9}$$

where I is the identity matrix. The functional $F_{M,T}$ can be rewritten as follows:

$$F_{M,T} = \int_{\Gamma^\pi} \left| (M - I)p + T + \delta(p) \right|^2 ds \tag{10}$$

The minimum of this functional corresponds to the zeros of its derivatives w.r.t. the motion parameters. After some calculation one obtains the following expressions of the transform parameters:

$$\begin{cases} \hat{M} &= -I_\Gamma^{-1} I_{\Gamma\delta} + I \\ \hat{T} &= -(\hat{M} - I)G_\Gamma - \overline{\delta}^\Gamma \end{cases} \tag{11}$$

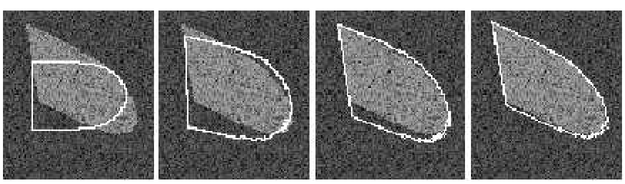

Figure 2: Affine registration of a contour on a synthetic image with Rayleigh statistics

where $G_\Gamma = (x_g^\Gamma, y_g^\Gamma)$ is the centroid of the contour and I_Γ its centered inertia matrix, $\overline{\delta}^\Gamma = (\overline{\delta}_x, \overline{\delta}_y)$ is the average of δ over the contour and the matrix $I_{\Gamma\delta}$ is defined as follows

$$I_{\Gamma\delta} = \int_{\Gamma^\pi} \begin{pmatrix} (x - x_g^\Gamma)(\delta_x - \overline{\delta}_x) & (y - y_g^\Gamma)(\delta_x - \overline{\delta}_x) \\ (x - x_g^\Gamma)(\delta_y - \overline{\delta}_y) & (y - y_g^\Gamma)(\delta_y - \overline{\delta}_y) \end{pmatrix} ds \tag{12}$$

These expressions are relatively simple and convenient for numerical implementation. Moreover, registration in this formulation does not require tuning of any weighting terms.

The affine registration problem is solved iteratively, until convergence. In order not to cumulate distortions of the contour due to numerical imprecisions, in each iteration the contour is transformed from its initial position (Γ_0^π, u_0^π) by a cumulated affine transform. The cumulated terms of the transform in iteration i ($M_c^{(i)}$, $T_c^{(i)}$) express as follows:

$$\begin{cases} M_c^{(i)} &= M^{(i)} M_c^{(i-1)} \\ T_c^{(i)} &= M^{(i)} T_c^{(i-1)} + T^{(i)} \end{cases} \tag{13}$$

where ($M^{(i)}$, $T^{(i)}$) are the transform parameters estimated at iteration i, and the initial cumulated values are $M_c^{(0)} = I$ (the identity matrix) and $T_c^{(0)} = 0$ (the null vector).

Figure 2 illustrates the performance of the algorithm on a synthetic image, whose statistics mimic the Rayleigh distributions of an echographic image. Initial position, two intermediate stages and the solution at convergence are shown.

3.1 Rigid registration

For the sake of echocardiographic data processing, we propose to further reduce the number of degrees of freedom of the model by introducing the rigid transform, performed in two consecutive steps: translation, and then rotation. As compared to affine registration, the rigid one is faster and less sensitive to noise, provided the motion to be recovered is approximately rigid.

If only translation is considered, the transform matrix $\hat{M}$ equals I (identity), and the resulting translation vector $\hat{T}$ is immediate from eq. 11:

$$\hat{T} = -\overline{\delta}^\Gamma \tag{14}$$

Considering pure rotation, the displacement writes:

$$v(p) = (R - I)p + T_G \tag{15}$$

where R is the rotation matrix about the angle θ:

$$R = \begin{pmatrix} \cos\theta & \sin\theta \\ -\sin\theta & \cos\theta \end{pmatrix} \tag{16}$$

and the vector T_G is such that the motion of the centroid G_Γ is null: $T_G = -(R - I)G_\Gamma$. Replacing in the cost functional (eq. 10) matrix M with the rotation matrix R, and deriving w.r.t. the motion parameter θ one obtains:

$$\tan\hat{\theta} = \frac{\int_\Gamma \left(x^*(\delta_x - x^*) - x^*(\delta_y - y^*) \right) ds}{\int_\Gamma \left(x^*(\delta_x - x^*) + y^*(\delta_y - y^*) \right) ds} \tag{17}$$

where $p^* = (x^*, y^*)$ denotes the position of point p in the coordinates of the centroid: $p^* = p - G_\Gamma$.

3.2 Prior displacement term

We now suppose the existence of an estimate of the displacement between the initial position of the contour Γ_0^π and the object to be segmented. This term expresses as a field $\eta = (\eta_x, \eta_y)$, defined over the entire image domain Ω and having meaningful values (w.r.t. the object motion) in the initial interior of Γ_0^π. This field could for example be obtained from a velocity estimation in a video sequence.

We propose to constrain the registration transform, so that it provides an inter-frame displacement close to η. We introduce this constraint into the cost functional (eq. 8) through a least square condition, with an anisotropic weight $\alpha = (\alpha_x, \alpha_y)$. The use of such a weight is motivated by the specificity of the ultrasound data, where acquisition and image properties in the two directions (axial and lateral) are fundamentally different.

The new functional is therefore formulated, with the additional displacement term calculated over the interior Ω_{in}^π, yielding the general expression:

$$F_{M,T} = \iint_{\Omega_{in}^\pi} \left(\alpha_x (v_x - \eta_x)^2 + \alpha_y (v_y - \eta_y)^2\right) d\omega + \int_{\Gamma^\pi} \left((1-\alpha_x)(v_x + \delta_x)^2 + (1-\alpha_y)(v_y + \delta_y)^2\right) ds \tag{18}$$

In the general case, the expression of the affine transform is quite complex and it is presented in the *Appendix*. In the current work, we use the displacement information only within the translation step, where the new translation vector writes as follows:

$$\begin{cases} T_x = \gamma_x^{-1}\left(S\alpha_x \overline{\eta_x}^\Omega - L(1-\alpha_x)\overline{\delta}_x^\Gamma\right) \\ T_y = \gamma_y^{-1}\left(S\alpha_y \overline{\eta_y}^\Omega - L(1-\alpha_y)\overline{\delta}_y^\Gamma\right) \end{cases} \tag{19}$$

with

$$\begin{cases} \gamma_x = (1-\alpha_x)L + \alpha_x S \\ \gamma_y = (1-\alpha_y)L + \alpha_y S \end{cases}$$

$\overline{\eta}^\Omega = (\overline{\eta}_x^\Omega, \overline{\eta}_y^\Omega)$ is the average of the term $\eta(p)$ calculated over the inside of the contour, and S is the area inside of the contour Γ^π.

In order to use $\overline{\eta}^\Omega$ within an iterative scheme, its expression has to be updated at each iteration i of the registration process. Indeed, this term is relative to the initial position of the contour Γ_0^π, and not to the position computed at the current iteration. In the case of translation, the updated displacement term $\tilde{\eta}^{\Omega(i)}$ at iteration i expresses as follows:

$$\tilde{\eta}^{\Omega(i)} = \overline{\eta}_0^{\Omega(i)} - T_c^{(i-1)} \tag{20}$$

where $\overline{\eta}_0$ is the value of the average estimated inside the initial position of the contour.

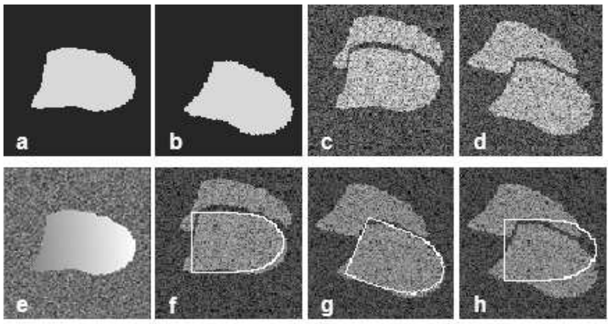

Figure 3: Rigid registration in a synthetic sequence with prior displacement term (see text)

To validate the framework, a synthetic sequence was constructed, where the object of interest was subject to translation and rotation. Fig. 3a,b show the positions of the object in frame 1 and in frame 2. To simulate the difficult conditions of an echographic image, a spurious shape was added in the vicinity of the object, and the obtained grayscale images are shown in fig. 3c,d. The axial displacement field was then calculated from the affine motion parameters used for the simulation (fig. 3e).

The registered position of the contour in frame 1 is shown in fig. 3f, and it is used as initial position for registration in frame 2. Fig. 3g,h present the result at convergence of rigid registration in frame 2, respectively with and without the axial displacement field introduced as prior. It is clear that in the presence of multiple objects, the prior displacement enables to correctly position the contour on the object of interest.

3.3 Application to echographic data

As indicated previously, rigid registration was used when processing echocardiographic data. Due to the specificity of the echographic image acquisition, only the axial velocities are currently available [5]. As a consequence, solely axial velocity information was introduced through the prior displacement term η_y, by setting $\alpha = (0, 1)$. Registration was performed on the non log-compressed envelope image, which is known to have Rayleigh statistics [10].

4 Segmentation

Let $u(p)$ be the evolving embedding function with its zero level set Γ. During the segmentation process, the registered prior shape (u^π, Γ^π) is used to constraint the motion of the zero level set. Given that $u^\pi(p)$ defines the minimum Euclidean distance between the point p and Γ^π, the quadratic attraction term acting on Γ is formulated as follows:

$$\chi^\pi(p \in \Gamma) = \begin{cases} 0 & , u^\pi(p) = 0 \\ +\left(u^\pi(p)\right)^2 & , u^\pi(p) > 0 \\ -\left(u^\pi(p)\right)^2 & , u^\pi(p) < 0 \end{cases} \tag{21}$$

One problem often encountered in segmentation of echocardiographic images is the attraction of the model by irrelevant structures, leading to completely erroneous solutions. The quadratic function, which allows relatively free motion of the contour in the vicinity of the prior shape while forbidding important amplitudes of motion, aims at reducing this effect.

A similar quadratic attraction term is introduced when segmenting temporal sequences of images, to ensure continuity between consecutive frames. Let $\{u^\tau\}, \tau = 0...N$ be the sequence of N embedding functions, each one acting on image I^τ from the sequence to be segmented. Level set u^τ is constraint by the level set $u^{\tau-1}$ with the following term:

$$\chi^{\tau,\tau-1}(p \in \Gamma^\tau) = \begin{cases} 0 & , u^{\tau-1}(p) = 0 \\ +\big(u^{\tau-1}(p)\big)^2 & , u^{\tau-1}(p) > 0 \\ -\big(u^{\tau-1}(p)\big)^2 & , u^{\tau-1}(p) < 0 \end{cases} \quad (22)$$

Since the two previously described terms, χ^π and $\chi^{\tau,\tau-1}$, are defined only on the zero level set of u, they are extended to the entire domain Ω in the following way:

$$\chi'(p) = \begin{cases} \chi(p) & \text{, if } p \in \Gamma \\ \chi(p_0)|\big(p_0 \in \Gamma \text{ and } \widehat{pp_0} = D(p,\Gamma)\big) & \text{, if } p \notin \Gamma \end{cases} \quad (23)$$

where $\widehat{pp_0}$ denotes the distance between p and p_0.

Figure 4 shows the segmentation of frame 2 from the previously presented synthetic sequence (fig. 3) using the proposed approach. The registered contour (as in fig. 3g) was used as initial and prior shape. Fig. 4a presents the result of segmentation after convergence, and in fig. 4b the same result is presented on a binary representation of the object of interest. Fig. 4c,d show the result obtained with no shape prior. One can see that the shape prior enables to correctly identify the object of interest in the presence of spurious structures on the image.

4.1 Application to echographic data

During the evolution of the level set, the classical curvature term κ is introduced to smooth the solution, and the region term is assumed to follow Rayleigh PDF.

The segmentation of the entire sequence was performed frame by frame. The complete evolution scheme expresses as follows:

$$\frac{du^\tau}{dt} = (\kappa + \lambda_\delta \delta_R + \lambda_\pi \chi'^\pi + \lambda_\chi \chi'^{\tau,\tau-1})|\nabla u| \quad (24)$$

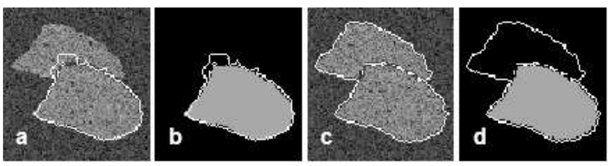

Figure 4: Segmentation of a synthetic image with (a, b) and without (c, d) shape prior

where δ_R is the region term based on Rayleigh statistics, and λ_δ, λ_π, λ_χ are weighting terms which enable to tune the influence of, respectively, the region term δ_R, the shape prior χ'^π and the temporal consistence term $\chi'^{\tau,\tau-1}$. Let us note that the solution was not observed to be very sensitive to these parameters.

5 Results in echographic data

Processed echocardiographic sequences were acquired using research ultrasound scanners equipped with a radio frequency (RF) output. The acquisition frame rates were high, in order to enable reliable estimation of the axial velocity. From the initial RF acquisition, two types of information were calculated: (1) the envelope image (2) the axial velocity field [5].

In this section, we present the different stages of processing and the final results in an apical four-chamber sequence acquired at 145 fps (fig. 1a). Results obtained in an apical four-chamber sequence acquired at 322 fps (fig. 1c) are subsequently shown. This latter sequence is particularly adapted for reliable calculation of tissue mechanical properties, and is therefore of a great medical interest. However, as a consequence of the very high frame rate, the acquisition angle is very narrow and the visual quality is extremely poor. The contrast between the muscle and blood is low, and the septum itself is difficult to identify in the images (see fig. 1c).

The sector reconstruction of the image, as seen in fig. 1, corresponds to the geometry of acquisition, and therefore presents the correct shape of the heart. However, processing was performed on images which were not sector reconstructed. For coherence, intermediate results will be presented on such rectangular images, and the final results will be sector reconstructed. As it is usually done in echography, the envelope images presented in this paper are log-compressed for visual assessment purposes. However, processing with the described algorithms was performed on the non-compressed envelope, which is known to have Rayleigh statistics [10, 9].

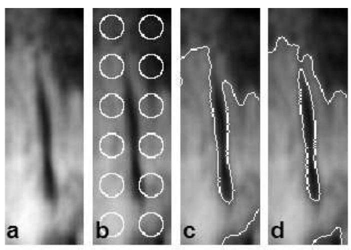

Figure 5: (a) the average velocity variance image, (b-d) initial, intermediate and final stage of segmentation

5.1 Construction of the shape prior

The issue of constructing the shape prior can be addressed in several ways. A common choice is to derive it from a set of training, expert segmented samples [22]. Another possibility is to manually trace the contour on one of the images from the sequence.

In the present work, we propose to derive the shape prior from the data set itself. In [6, 7], we described a method for cardiac muscle detection based on the variance of the axial velocity field (subsequently called ξ_v). Here, we introduce an original approach, where the sequence of images is considered as a single multichannel image, representing several acquisitions of the same object. Indeed, the heart muscle has a cyclic motion, whose amplitude does not exceed by far the size of the muscle itself. Consequently, it stays within a constrained region of the image. The goal of extracting a prior shape thus reduces to identifying this region.

Inspired by the work of Germain and Refregier [8], we propose to process the multichannel image by segmenting a unique image, which is the average of all the channels. Segmentation was performed using a conventional, region driven level set evolution as given by:

$$\frac{du}{dt} = (\kappa + \lambda_\delta \delta_G)|\nabla u| \tag{25}$$

where the statistics were assumed to be Gaussian. Fig. 5a shows the average $\overline{\xi}_v$ of ξ_v from all the frames of the sequence, and 5b-d show the initial, an intermediate and the final stage of the level set evolution on this image. The parameters of the Gaussian distribution were estimated in the maximum a posteriori sense, that is re-estimated after each iteration. Several candidate regions resulted from the segmentation, and the one corresponding to the septum was chosen manually.

The partition resulting from a similar segmentation of the average of the envelope images was used to derive statistical properties of the regions in each envelope image. The obtained statistical parameters of the Rayleigh distribution were used both in the registration and the segmentation step.

5.2 Registration and segmentation

Registration was performed frame by frame, taking the solution of frame $\tau - 1$ as initial position for frame τ. After the registration step was complete, frame by frame segmentation was performed. In each frame, the registered contour served both as initial shape and as shape prior for the evolving level set.

Fig. 6 shows, in one frame, all the steps of the segmentation algorithm: the initial position of the shape prior, the position of the shape prior after translation, after rotation and the final result of segmentation with the shape prior. The interest of using the axial displacement information in the registration step is illustrated in fig. 7, in three frames extracted from the sequence. When taking into account the axial displacement, the axial motion of the septum is correctly

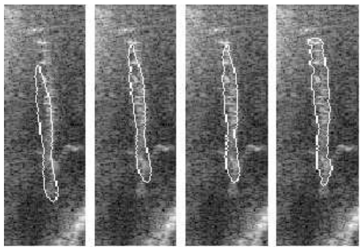

Figure 6: The different stages of the algorithm shown in one frame: initial contour, translation, rotation, final segmentation

resolved (fig. 7a-c). To the contrary, registration without this displacement prior does not allow correct axial tracking of the muscle (fig. 7d-f, a dotted line indicates the position of the contour in the first frame).

Fig. 8 shows segmented frames extracted from the sequence. In all of them, the contour matches the muscle very well. It is particularly encouraging that segmentation is correct in the upper part of all the images, where contrast is extremely poor due to the ultrasonic near field. One can appreciate how the contour moves, rotates and bends along with the contracting muscle. Frame 149 corresponds in the next cardiac cycle to the same instant as frame 4. The detected contours are almost identical in the two frames, proving stability of the algorithm and repeatability of the results.

5.3 Application to very high frame rate acquisition

Fig. 9 shows the results of segmentation obtained in an apical four-chamber sequence acquired at a very high frame rate. The segmentation procedure was similar to the one described previously. The axial and lateral motion as well as rotation of the muscle can be clearly seen in the images. Frame 327 corresponds in the next cardiac cycle to frame 5: the segmented contours have very similar shapes and positions, proving again a high stability of the algorithm. In frame 164 (and neighboring frames in the sequence), where the contour is at its highest position in the image, the upper part of the contour tends to drift in the direction of the apex, due to the very high intensity of the near field.

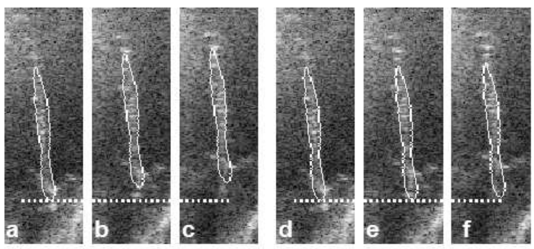

Figure 7: Result of translation in three frames: (a-c) axial velocity taken into account during registration, (d-f) no axial velocity taken into account

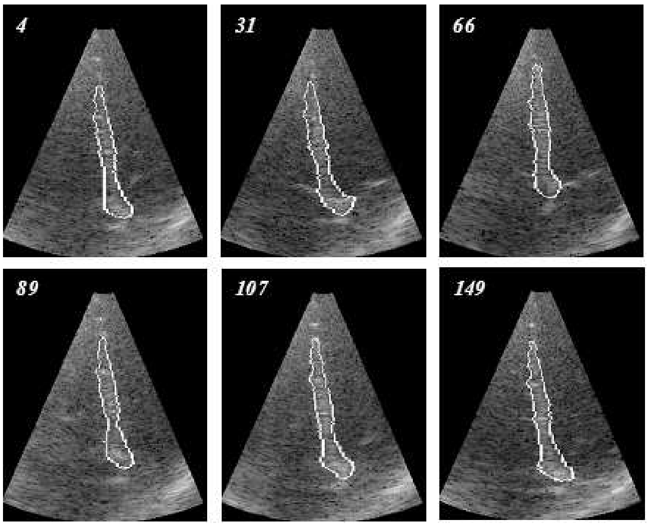

Figure 8: Result of segmentation on six frames extracted from the sequence (numbers indicate frame position in the sequence)

These results show that the method performs correctly even in very difficult images. It is definitely the dispmacement information, introduced in the rigid registration step, which allows to resolve the axial position of the septum.

6 Conclusion

In this paper, we have proposed a scheme for introducing motion, shape and position priors in the level set representation. An affine registration algorithm has been developed within a variational framework, which include the constraint of an external displacement field. One advantage of the proposed method is that the same formulation of the region information is used both for registration and segmentation.

Encouraging results were obtained in two entire cardiac echographic sequence. Until now, very few work have used level sets on ultrasound images, because of their poor visual quality as compared to other imaging modalities. It appears that segmentation of medical echographic data in the level set framework requires additional prior knowledge, and the present work proposes a method to overcome this limitation.

Segmentation with our algorithm yields the following results: (1) the affine registration parameters, (2) the evolved level sets. From this information, the motion field can be readily estimated, and it can be used to respond to the medical objective behind this work, that is region tracking in echographic sequences.

Future development of this work includes integrating registration and segmentation within a unique level set evolution scheme, resulting in a robust segmentation algorithm.

As a last point, it is to be noted that recent research in the field of ultrasonic RF signal processing aims at obtaining the lateral component of the muscle velocity [11], in addition to the already available axial component. Estimated lateral displacement could also be taken into account in the registration framework, to accurately position the shape on the moving muscle.

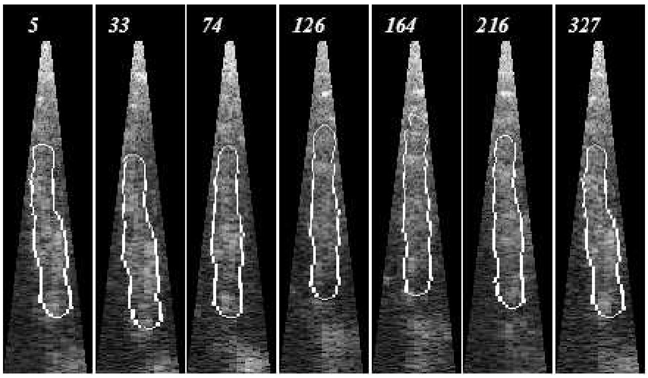

Figure 9: Results of segmentation obtained in a very high frame rate acquisition

Acknowledgements

The authors would like to thank Bart Bijnens and Jan D'hooge from Cardiac Ultrasound Research, University Hospital of Leuven, Belgium, for providing specific ultrasound data and fruitful discussions. The authors would also like to thank Fadi Jamal, cardiologist from the Cardiologic Hospital Louis Pradel, Lyon, France, for his expert comments which greatly improved the medical contents of this work.

Appendix

Derivation of the affine transform parameters for the complete criterion, including image-based and external displacement constraints as formalized in eq. 18, yields the following equations:

$$\begin{cases} \hat{M} & = -\overline{I}_G^{-1}(\overline{I}_\delta - \overline{I}_\eta) + I \\ \hat{T} & = -\gamma'((\hat{M} - I)\overline{G}_{diag} + \tilde{\delta} - \tilde{\eta}) \end{cases} \tag{26}$$

The column vector and the matrix of the weighted centroid are

$$\overline{G}_{diag} = \begin{pmatrix} G_{xx} \\ G_{yy} \end{pmatrix} \qquad \overline{G} = \begin{pmatrix} G_{xx} & G_{xy} \\ G_{yx} & G_{yy} \end{pmatrix} \tag{27}$$

with

$$G_{ij} = (1 - \alpha_i) L j_g^\Gamma + \alpha_i S j_g^\Omega \tag{28}$$

where i, j stand for x or y, L, S are respectively the length and surface of the contour, and $G^\Gamma = (x_g^\Gamma, y_g^\Gamma)$, $G^\Omega = (x_g^\Omega, y_g^\Omega)$ are the centroids of the contour Γ and the region Ω_{in}, respectively. The weighted inertia matrix $\overline{I}_G$ expresses as follows

$$\overline{I}_G = \begin{pmatrix} \overline{I}_{G/xx} & \overline{I}_{G/xy} \\ \overline{I}_{G/yx} & \overline{I}_{G/yy} \end{pmatrix} \tag{29}$$

with

$$\overline{I}_{G/ij} = (1-\alpha_i)\int_{\Gamma^\pi} ijds + \alpha_i \iint_{\Omega_{in}^\pi} ijd\omega - \frac{\overline{G}_{ij}\overline{G}_{ii}}{\gamma_i} \quad (30)$$

The term $\overline{I}_\delta$ is

$$\overline{I}_\delta = \begin{pmatrix} \overline{I}_{\delta/xx} & \overline{I}_{\delta/xy} \\ \overline{I}_{\delta/yx} & \overline{I}_{\delta/yy} \end{pmatrix} \quad (31)$$

with

$$\overline{I}_{\delta/ij} = (1-\alpha_i)\int_{\Gamma^\pi} \delta_i jds - \frac{\tilde{\delta}_i \overline{G}_{ij}}{\gamma_i} \quad (32)$$

The term $\overline{I}_\eta$ expresses as

$$\overline{I}_\eta = \begin{pmatrix} \overline{I}_{\eta/xx} & \overline{I}_{\eta/xy} \\ \overline{I}_{\eta/yx} & \overline{I}_{\eta/yy} \end{pmatrix} \quad (33)$$

with

$$\overline{I}_{\eta/ij} = (1-\alpha_i)\iint_{\Omega_{in}^\pi} \eta_i jd\omega - \frac{\tilde{\eta}_i \overline{G}_{ij}}{\gamma_i} \quad (34)$$

where $\tilde{\delta}^\Gamma = (\tilde{\delta}_x, \tilde{\delta}_y)$ is

$$\tilde{\delta}^\Gamma = \begin{pmatrix} (1-\alpha_x) & 0 \\ 0 & (1-\alpha_y) \end{pmatrix} \int_{\Gamma^\pi} \delta ds \quad (35)$$

and $\tilde{\eta}^\Omega = (\tilde{\eta}_x, \tilde{\eta}_y)$ is

$$\tilde{\eta}^\Omega = \begin{pmatrix} \alpha_x & 0 \\ 0 & \alpha_y \end{pmatrix} \iint_{\Omega_{in}^\pi} \eta d\omega \quad (36)$$

The generalized weighting vector $\gamma = (\gamma_x, \gamma_y)$ expresses as

$$\gamma = (1-\alpha)L + \alpha S \quad (37)$$

(1 stands for the column vector $(1,1)$) and the generalized inverse weight matrix is defined as

$$\gamma' = \begin{pmatrix} \gamma_x^{-1} & 0 \\ 0 & \gamma_y^{-1} \end{pmatrix} \quad (38)$$

References

[1] C. Baillard and C.Barillot. Robust 3d segmentation of anatomical structures with level sets. In *MICCAI*, pages 236–245, 2000.

[2] D. Boukerroui, O. Basset, A. Baskurt, and G. Gimenez. A multiparametric and multiresolution segmentation algorithm of 3-d ultrasonic data. *IEEE Trans UFFC*, 48(1):64–77, 2001.

[3] T. F. Chan and L. A. Vese. Active contours without edges. *IEEE Trans Im Proc*, 10(2):266–277, 2001.

[4] Y. Chen, H. D. Tagare, S. Thiruvenkadam, F. Huang, D. Wilson, K. S. Gopinath, R. W. Briggs, and E. A. Geiser. Using prior shapes in geometric active contours in a variational framework. *International Journal of Computer Vision*, 50(3):315–328, 2002.

[5] J. D'hooge, E. Konofagou, F. Jamal, A. Heimdal, L. Barrios, B. Bijnens, J. Thoen, F. Van de Werf, G. Sutherland, and P. Suetens. Two-dimensional ultrasonic strain rate measurement of the human heart in vivo. *IEEE Trans UFFC*, 49(2):281–286, 2002.

[6] I. Dydenko, S. Chehbi, D. Friboulet, P. Clarysse, J. D'hooge, B.Bijnens, and I. E. Magnin. Using an elastic deformable template for the segmentation of ultrasound cardiac radio frequency images based on the velocity information. In *IEEE UFFC Symposium*, pages 1706–1709, 2002.

[7] I. Dydenko, D. Friboulet, J.-M. Gorce, J. D'hooge, B.Bijnens, and I. E. Magnin. Towards ultrasound cardiac image segmentation based on the radiofrequency signal. *Med Image Ana*, to be published, 2003.

[8] O. Germain and P. Refregier. Snake-based method for the segmentation of object in mulitchannel images degraded by speckle. *Optics letters*, 24(12):814–816, 1999.

[9] G. Guerault, P. Delachartre, G. Finet, and I. E. Magnin. Modélisation et segmentation d'images échographiques endovasculaires. *Traitement du Signal*, 17(5-6):517–529, 2000.

[10] D. Kaplan and A. Ma. On the statistical characteristcs of log-compressed rayleigh signals. In *IEEE Ultrasonics Symposium*, 1993.

[11] S. Langeland, J. D'hooge, H. Torp, B. Bijnens, and P. Suetens. A simulation study of the performance of different estimators for two-dimensional velocity estimation. In *IEEE UFFC Symposium*, pages 1815–1818, 2002.

[12] M. Leventon, E. Grimson, and O. Faugeras. Statistical shape influence in geodesic active contours. In *Comp. Vision and Patt. Recon. (CVPR)*, 2000.

[13] M. E. Leventon, O. Faugeras, W. E. L. Grimson, and W. M. W. III. Level set based segmentitation with intensity and curvature priors. In *IEEE Workshop on Mathematical Methods in Biomedical Image Analysis (MMBIA'00)*, 2000.

[14] N. Lin, W. Yu, and J. S. Duncan. Combinative multi-scale level set framework for echocardiographic image segmentation. In *MICCAI*, pages 682–689, 2002.

[15] I. Mikic, S. Krucinski, and J. D. Thomas. Segmentation and tracking in echocardiographic sequences: active contours guided by optical flow estimates. *IEEE Trans Med Imaging*, 17(2):274–284, 1998.

[16] V. Moreau, L. D. Cohen, and D. Pellerin. Deformation field estimation for the cardiac wall using doppler tissue imaging. In *Functional Imaging and Modeling of the Heart*, pages 53–60, 2001.

[17] M. Mulet-Parada and J. A. Noble. 2d+t acoustic boundary detection in echocardiography. *Med Image Anal*, 4:21–30, 2000.

[18] S. Osher and J. A. Sethian. Front propagating with curvature dependent speed: algorithms based on hamilton-jacobi formulations. *Journal of computational physics*, 79:12–49, 1988.

[19] N. Paragios and R. Deriche. Geodesic active regions for motion estimation and tracking. Technical Report 3631, INRIA, 1999.

[20] N. Paragios and R. Deriche. Geodesic active regions for supervised textural segmentation. In *IEEE ICCV*, pages 926–938, 1999.

[21] S. I. Rabben, A. H. Torp, A. Stoylen, S. Slordahl, K. Bjornstad, B. O. Haugen, and B. Angelsen. Semiautomatic contour detection in ultrasound m-mode images. *Ultrasound Med Biol*, 26(2):287–296, 2000.

[22] M. Rousson and R. Deriche. A variational framework for active and adaptive segmentation of vector valued image. Technical Report 4515, INRIA, 2002.

[23] C. Samson, L. Blanc-Fraud, G. Aubert, and J. Zerubia. A level set method for image classification. In *Int Conf Scale-Space Theories in Computer Vision*, pages 306–317, 1999.

[24] A. Tsai, A. Yezzi, W. Wells, C. Tempany, D. Tucker, A. Fan, A. Grimson, and A. Willsky. Model-based curve evolution technique for image segmentation. In *IEEE CVPR*, 2001.

[25] A. Yezzi, L. Zollei, and T. Kapur. A variational framework for integrating segmentation and registration through active contours. *Med Image Ana*, 7:171–185, 2003.

[26] S. C. Zhu and A. Yuille. Region competition: Unifying snakes, region growing and bayes/mdl for multi-band image segmentation. *IEEE Trans.on Pattern Analysis and Machine Intelligence*, 18(9):884–900, 1996.